

The Role of Bridging Ligands in Controlling Electronic and Magnetic Properties in Polynuclear Complexes

JON A. MCCLEVERTY* AND
MICHAEL D. WARD*

School of Chemistry, University of Bristol, Cantocks Close,
Bristol BS8 1TS, U.K.

Received May 7, 1998

Introduction

The ability to control electronic and magnetic interactions between metal centers across a bridging ligand is of fundamental importance in inorganic and materials chemistry. An electronic interaction between two (usually chemically equivalent) metal centers is manifested by a separation between their redox potentials, such that in the intermediate potential domain the complex exists in a mixed-valence state and can undergo optically induced intervalence electron transfer.¹ The significance of this is 2-fold. First, the most fundamental process in chemistry, electron transfer, may be studied under controlled *intramolecular* conditions: across a fixed distance, between fragments of known properties, and through a conduit whose conformation and electronic characteristics are well-defined. This contrasts with the situation for *intermolecular* electron transfer, where the separation, conformation, and relative orientation of the interacting complexes at the moment of collision are difficult to know accurately. Second, the ability of long, conjugated bridging ligands to act as “molecular wires” for possible use in molecular electronic devices may be evaluated, because the ability of a bridging ligand to mediate *transfer* of one electron across it within a molecule may be a reasonable guide to its ability to permit *transport* of electrons across it in a nanoscopic circuit.² Consequently the study of electronic interactions between metal ions as a function of the bridging ligand properties is a well-researched field.¹

Magnetic exchange interactions between metals in dinuclear (or larger) complexes are likewise dependent on the nature of the pathway linking the metal ions.³ If the metal-based magnetic orbitals are sufficiently close to overlap directly, then the sign of the magnetic interaction depends on their relative symmetry, as formalized in the Goodenough–Kanamori rules.⁴ This has been exploited in the preparation of complexes with predictable magnetic properties (Figure 1).^{3,5} If however the magnetic orbitals

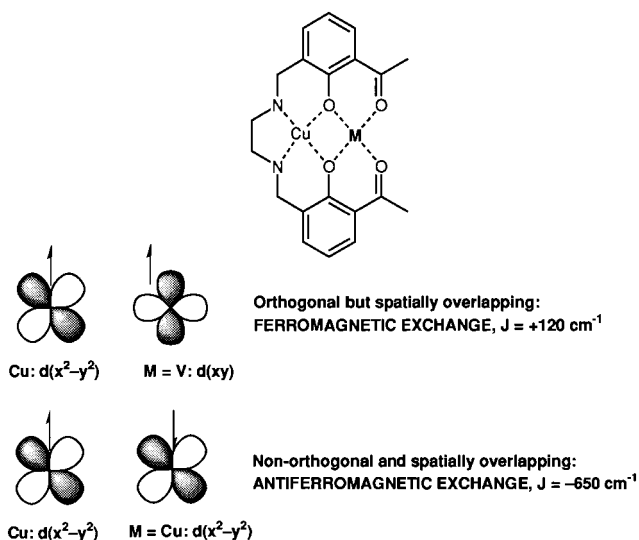


FIGURE 1. Effect of mutual orientation of overlapping magnetic orbitals on the sign of the exchange interaction [from ref 5a].

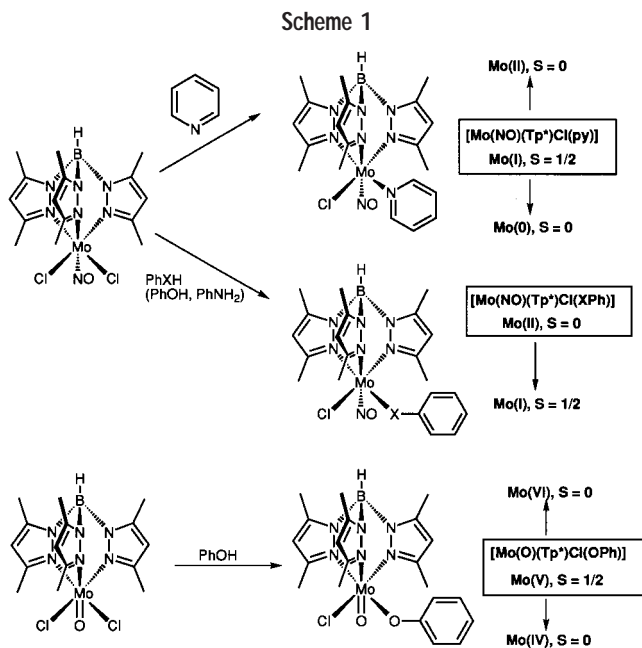
are too far apart to overlap directly, but require the participation of bridging ligand orbitals to mediate the interaction (a superexchange process), then the properties of the bridging ligand will become as important as they are in mediating electronic interactions. This principle has received relatively little systematic attention for metal complexes, in contrast to the extensive work on the magnetic properties of organic polyradicals as a function of structure and topology.⁶ This is surprising considering the obvious advantages of metal-based radicals over organic radicals for use in magnetic materials: higher spin density in many cases, chemical stability, and the possibility of redox activity for switching purposes. The ability to design desirable properties into magnetic materials by control of the bridging pathways at the construction stage has obvious appeal.

Accordingly, we have been interested in evaluating both electronic and magnetic interactions between metal centers across a range of bridging ligands designed to allow study of the effects of ligand length, conformation, and topology.

The Building Blocks

For this work we used two metal complex fragments: $\{\text{Mo}(\text{NO})\text{Tp}^*\text{X}\}$ ($\text{X} = \text{halide}$) in which the Mo is usually in oxidation state +1 (d^5 configuration), (for oxidation state assignment, the nitrosyl ligand is formally represented as NO^+ so that the $\{\text{Mo}(\text{NO})\}^{2+}$ core, as in $[\text{Mo}(\text{NO})\text{Tp}^*\text{Cl}(\text{py})]$, contains d^5 Mo(I)), and $\{\text{Mo}(\text{O})\text{Tp}^*\text{Cl}\}$, in which the Mo is usually in oxidation state +5 (d^1 configuration) [Tp^* is hydrotris(3,5-dimethylpyrazolyl)borate]. The basic chemistry of these fragments is outlined in Scheme 1. The $\{\text{Mo}(\text{NO})\text{Tp}^*\text{Cl}\}$ unit forms neutral paramagnetic 17-electron $[\text{Mo}(\text{I})]$ complexes with pyridine as the sixth ligand, and neutral diamagnetic 16-electron $[\text{Mo}(\text{II})]$ complexes with phenolates or aromatic amides as the sixth ligand.⁷ The $\{\text{Mo}(\text{O})\text{Tp}^*\text{Cl}\}$ unit forms neutral paramagnetic Mo(V)

Jon A. McCleverty is Professor and Michael D. Ward is a Reader in the inorganic chemistry section at the University of Bristol.



complexes with phenolate as the sixth ligand.⁸ By use of appropriate bridging ligands containing two or more pyridyl or phenolate termini, polynuclear complexes incorporating these metal fragments can be prepared.

Despite the difference in the formal oxidation states of the $\{\text{Mo}^{\text{I}}(\text{NO})\text{Tp}^*\text{Cl}\}$ and $\{\text{Mo}^{\text{V}}(\text{O})\text{Tp}^*\text{Cl}\}$ fragments, their electrochemical and magnetic properties are comparable for two reasons. First, the unpaired electron is in the d_{xy} orbital in each case (Figure 2). In the former case the NO ligand is a *strong* π -acceptor: taking the Mo–NO axis as the z -axis, the two empty NO π^* orbitals overlap with the d_{xz} and d_{yz} metal orbitals, thereby lowering them, but leaving d_{xy} unchanged. The Mo(I) electron configuration is therefore $d_{xz}^2d_{yz}^2d_{xy}^1$. In the latter case the oxo ligand is a *strong* π -donor: the filled oxygen p_x and p_y orbitals overlap with the metal d_{xz} and d_{yz} orbitals, thereby raising them, but leaving d_{xy} unchanged. The Mo(V) electron configuration is therefore $d_{xy}^1d_{xz}^0d_{yz}^0$. In each case the magnetic orbital is of the correct symmetry for $d(\pi)$ – $p(\pi)$ overlap with the bridging ligand. Second, the strongly electron-withdrawing nature of the NO ligand attached to Mo(I), and the strongly electron-donating nature of the oxo ligand attached to Mo(V), means that the actual electron densities at the metal centers are likely to be comparable.⁹

A combination of several factors makes these two metal fragments ideal for our purposes. Both are paramagnetic (enabling study of magnetic exchange interactions by magnetic susceptibility and EPR spectroscopic measurements) and redox active (enabling study of electronic interactions by voltammetry). The favorable interaction between the d_{xy} orbital—which is both the magnetic orbital, and the frontier orbital where redox interconversions are based—with the bridging ligand π -system means that ligand-mediated interactions between the metal centers are exceptionally strong (see later). The Mo–NO group and the Mo=O groups provide strong IR peaks which are convenient spectroscopic handles for monitor-

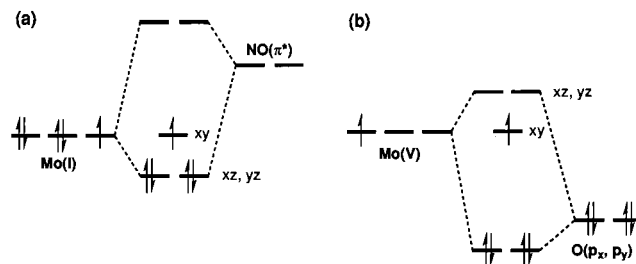


FIGURE 2. Ground-state electron configurations for complexes based on (a) $\{\text{Mo}^{\text{I}}(\text{NO})\text{Tp}^*\text{Cl}\}$ and (b) $\{\text{Mo}^{\text{V}}(\text{O})\text{Tp}^*\text{Cl}\}$ fragments.

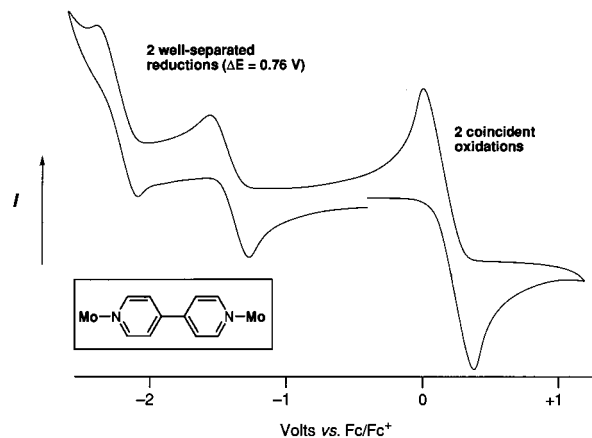


FIGURE 3. Cyclic voltammogram of $\{[\text{Mo}^{\text{I}}(\text{NO})\text{Tp}^*\text{Cl}]_2(\mu\text{-}4,4'\text{-bpy})\}$ showing well-separated one-electron Mo(I)/Mo(0) reductions and coincident Mo(I)/Mo(II) oxidations.



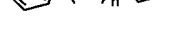

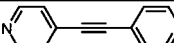
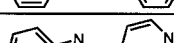
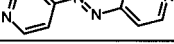
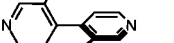
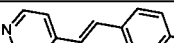
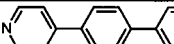
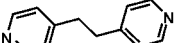
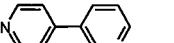
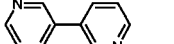
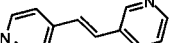
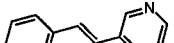
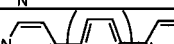
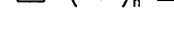
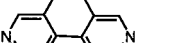
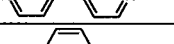
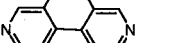
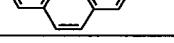
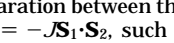

ing changes in electron density at the metal center. Finally the synthetic chemistry of the $\{\text{Mo}^{\text{I}}(\text{NO})\text{Tp}^*\}$ and $\{\text{Mo}^{\text{V}}(\text{O})\text{Tp}^*\}$ fragments is well established.

Electronic Interactions

Nitrosyl–Mo(I) Complexes with Bispyridyl Bridging Ligands. The first complex of this series was $\{[\text{Mo}^{\text{I}}(\text{NO})\text{Tp}^*\text{Cl}]_2(\mu\text{-}4,4'\text{-bipy})\}$ (**2**; bipy = bipyridyl).¹⁰ Its cyclic voltammogram (Figure 3) showed that the two chemically reversible reductions, formally Mo(I)/Mo(0) couples, were separated by 765 mV; in contrast the two oxidations, formally Mo(I)/Mo(II) couples, were essentially coincident. The $\Delta E_{1/2}$ value of 765 mV represents an unprecedentedly large interaction across a bridging ligand of this length: for example, in $\{[\text{Ru}(\text{NH}_3)_5]_2(\mu\text{-}4,4'\text{-bipy})\}^{4+/5+/6+}$ the Ru(II)/Ru(III) couples are separated by 76 mV, 1/10 as much.¹¹ Examination of many such complexes with bispyridyl bridging ligands was therefore carried out, and the results are summarized in Table 1.^{10,12–17} In all cases a separation is observed between the reductions, but the oxidations are coincident except in one case. The single exception is with the monocyclic bridging ligand pyrazine (**1**), which gives a huge separation of 1440 mV between the Mo(I)/Mo(0) reductions [*cf.* $\Delta E_{1/2} = 370$ mV for the Creutz–Taube ion,¹⁸ which has the same bridging ligand] and, remarkably, a separation of 100 mV between the Mo(I)/Mo(II) oxidations.

The effects of increasing ligand length are clear, and in the series of bis(4-pyridyl)polyene-bridged complexes (**2**–**7**) the decrease in $\Delta E_{1/2}$ as the number of C=C spacers

Table 1. Electrochemical and Magnetic Interactions between {Mo(NO)(Tp^{*})Cl} Fragments Across Bis-pyridyl Bridging Ligands

Complex	Bridging ligand L in [{Mo(NO)(Tp [*])Cl} ₂ (μ-L)]	$\Delta E_{1/2}$ (mV) ^a	Ref	J (cm ⁻¹) ^b	Ref
1		1440	13		
2		n = 0 765	10	-33	15
3		n = 1 582	10	-18	15
4		n = 2 390	12		
5		n = 3 230	12		
6		n = 4 110	12		
7		n = 5 36	12		
8		560	14		
9		500	14		
10		380	14	-3.5	17
11		160	14		
12		260	14		
13		105	10		
14		460	15	+0.8	15
15		210	15	-1.5	15
16		490	15	+2.4	15
17		190	15	-1.5	15
18		n = 1 450	16		
19		n = 2 220	16		
20		n = 3 60	16		
21		n = 4 not resolved	16		
22		790	17	-36	17
23		730	17	-35	17

^a Separation between the two Mo(I)/Mo(0) couples. ^b J is defined from $H = -J\mathbf{S}_1 \cdot \mathbf{S}_2$, such that negative J denotes antiferromagnetism and positive J denotes ferromagnetism.

increases is nearly linear up to four double bonds [Figure 4a]. Imposing a twist between the two pyridyl rings by using 3,3'-dimethyl-4,4'-bipy as the bridge (compare **2** and **10**) decreases $\Delta E_{1/2}$ by 50%, and $\Delta E_{1/2}$ also decreases when 4-pyridyl groups are replaced by 3-pyridyl groups (compare **2** with **14** and **15**, and **3** with **16** and **17**), consistent with the findings of others that *meta*-substituted aromatic rings are less effective at transmitting electron interactions.¹⁹ Addition of saturated spacers such as $-\text{CH}_2\text{CH}_2-$ results in a dramatic decrease in $\Delta E_{1/2}$ (**13**). All of these trends are what would be expected if the electronic interaction were transmitted principally by delocalization across the π -system of the bridging ligand, but nonetheless the exceptional strength of the interaction between the

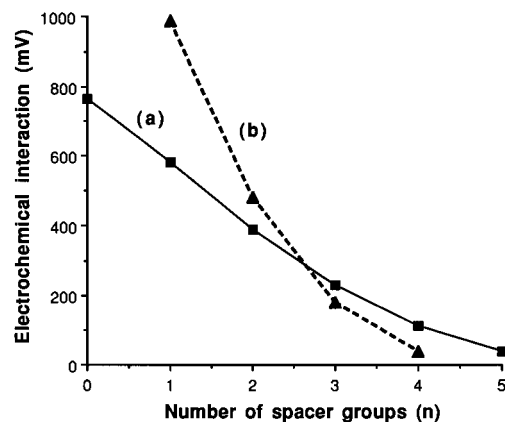


FIGURE 4. Electrochemical interactions as a function of ligand length: separation between (a) Mo(I)/Mo(0) couples in $\{[\text{Mo}^{\text{I}}(\text{NO})\text{Tp}^*\text{Cl}]_2(\mu\text{-NN})\}$ where NN is $\text{py}-(\text{CH}=\text{CH})_n\text{-py}$ ($n = 0-4$) and (b) Mo(V)/Mo(VI) couples in $\{[\text{Mo}^{\text{V}}(\text{O})\text{Tp}^*\text{Cl}]_2(\mu\text{-OO})\}$, where OO is $[\text{O}(\text{C}_6\text{H}_4)_n\text{O}]^{2-}$ ($n = 1-4$).

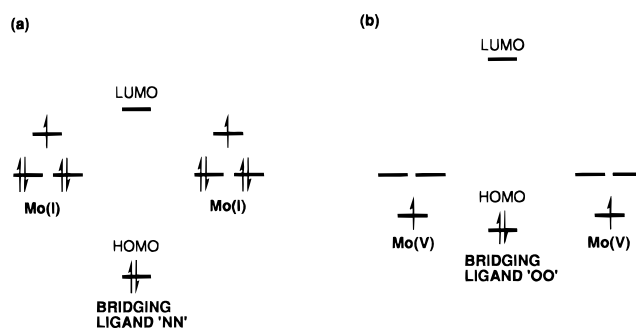
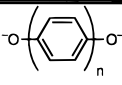
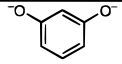
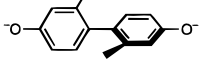


FIGURE 5. Qualitative MO scheme for (a) dinuclear complexes $\{[\text{Mo}^{\text{I}}(\text{NO})\text{Tp}^*\text{Cl}]_2(\mu\text{-NN})\}$ (NN = bispyridyl bridge) and (b) dinuclear complexes $\{[\text{Mo}^{\text{V}}(\text{O})\text{Tp}^*\text{Cl}]_2(\mu\text{-OO})\}$ (OO = bisphenol bridge).

Mo(I)/Mo(0) couples makes it particularly easy to measure interactions even across relatively long bridges.

Given this large interaction between the Mo(I)/Mo(0) couples, why are the Mo(I)/Mo(II) couples coincident? A plausible answer is in Figure 5a. The relatively high-energy d_{xy} orbitals are not far below the low-lying π^* orbitals of the bipyridyl bridging ligand, over which delocalization can occur. Addition of a second electron to each d_{xy} orbital will raise them in energy nearer to the π^* level, such that on reduction the d_{xy} electrons are delocalized even more effectively across the bridge. One can therefore write $\{\text{Mo}(\text{0})-\text{L}-\text{Mo}(\text{0})\}$ and $\{\text{Mo}(\text{I})-[\text{L}^{2-}]-\text{Mo}(\text{I})\}$ as the two extreme forms of the doubly reduced species, consistent with the known ability of polypyridine ligands to be reduced easily. Since the two additional electrons are brought together by this process, the electrostatic repulsion between them will be strong, making addition of the second electron much more difficult than addition of the first—hence the large $\Delta E_{1/2}$ values. In contrast, oxidation of the metals and the resultant positive charge will lower the d_{xy} orbitals away from the π^* levels such that the d_{xy} electrons are more metal-localized. Also, the HOMO of the bridging ligand is much lower than the d_{xy} orbitals and therefore cannot participate in stabilizing the oxidized species: i.e., the doubly-oxidized form $\{\text{Mo}(\text{II})-\text{L}-\text{Mo}(\text{II})\}$ will not have any significant contribution

Table 2. Electrochemical (ref 20) and Magnetic (ref 17) Interactions between {MoO(Tp*)Cl} Fragments across Bisphenolate Bridging Ligands

Complex	Bridging ligand L in [{MoO(Tp*)Cl} ₂ (μ-L)]	$\Delta E_{1/2}$ (mV) ^a	J (cm ⁻¹) ^b
24	 $n = 1$ $n = 2$ $n = 3$ $n = 4$	990	-80
25		480	-13.2
26		180	
27		not resolved	
28		N/A	+9.8
29		230	-2.8

^a $\Delta E_{1/2}$ is the separation between the two Mo(V)/Mo(VI) couples.

^b J is defined from $H = -JS_1 \cdot S_2$, such that negative J denotes antiferromagnetism and positive J denotes ferromagnetism.

from the {Mo(I)–[L²⁺]-Mo(I)} form in which the oxidations are partly ligand-centered.

Oxo–Mo(V) Complexes with Bisphenolate Bridging Ligands. The series of complexes of the form [{Mo(O)Tp*Cl}₂(μ-OO)], where the dianionic bridging ligands “OO” are listed in Table 2, were studied in the same way (see also Figure 6).²⁰ The mononuclear complex [Mo(O)Tp*Cl(OPh)] undergoes reversible Mo(V)/Mo(VI) and Mo(V)/Mo(IV) couples, so for the dinuclear complexes we expected to see two oxidations and two reductions in their voltammograms, and this was confirmed (Table 2).²⁰ The unusual feature of the electrochemical behavior was that whereas the two Mo(V)/Mo(VI) oxidations were very widely separated, the Mo(V)/Mo(IV) reductions were coincident for all but the shortest bridging ligand, exactly the opposite of the pattern observed for the Mo(I)–NO complexes described above. Again the $\Delta E_{1/2}$ values between the Mo(V)/Mo(VI) couples vary in a manner consistent with the electronic interaction being transmitted through the π -system of the bridging ligand: $\Delta E_{1/2}$ decreases with (i) increasing length of the bridging ligand [24–27; Figure 4b], (ii) changing the substitution pattern from *para* to *meta* (compare 24 and 28), and (iii) enforcing a 90° twist between two aromatic rings in the bridge (compare 25 and 29).

The presence of a strong interaction between the oxidations, but not between the reductions, is explained in Figure 5b. The d_{xy} orbital, being the lowest in energy of the metal d orbitals, is not far above the HOMO of the diphenol bridging ligand, which is relatively high in energy because of its double negative charge. Oxidation will lower the d_{xy} orbitals further, and the positive charges will therefore be partly delocalized onto the bridging ligand. In contrast reduction to Mo(IV) will raise the d_{xy} orbitals away from the bridging ligand HOMO such that delocalization is decreased, and the bridging ligand LUMO is too high in energy to participate, so the reductions are metal-localized. Thus, for the doubly-oxidized species one can write {Mo(VI)–[OO]²⁻–Mo(VI)} and {Mo(V)–[OO]–Mo(V)} as extreme canonical forms, and of course the fact that oxidation of the bridging ligand is a significant contributor is consistent with the known tendency of

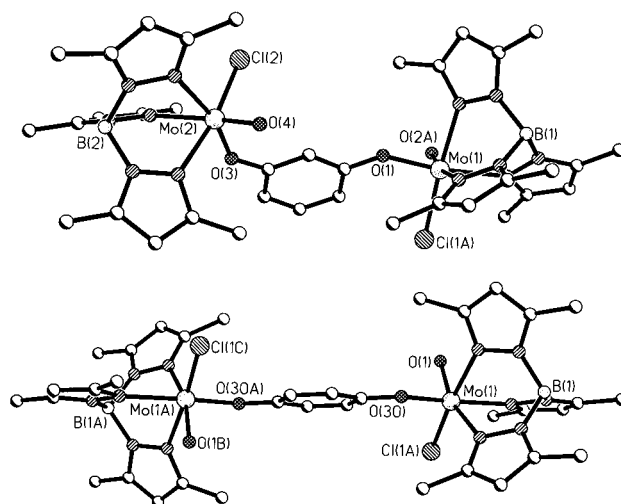


FIGURE 6. Crystal structures of 28 (top) and 24 (bottom).

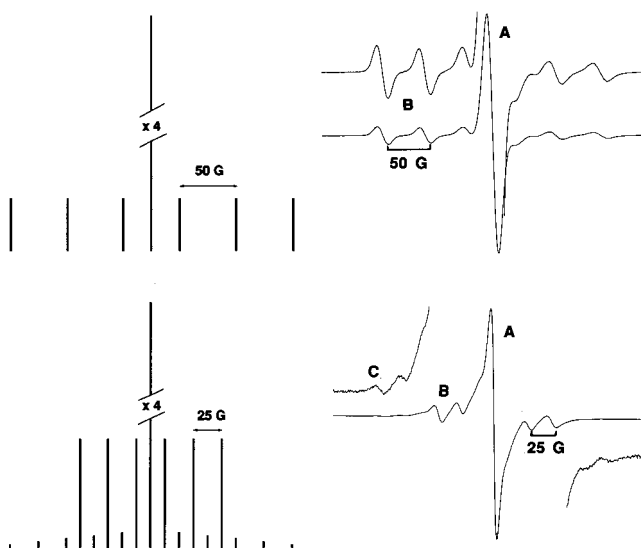


FIGURE 7. Idealized and real EPR spectra for (top) mononuclear molybdenum complexes and (bottom) dinuclear molybdenum complexes in which $|J| \gg A_{Mo}$.

para-substituted diphenols to be oxidized to quinones. It is significant that, with the *meta*-substituted bridge (28), in which no quinonoidal form is possible, only a single totally irreversible oxidation occurs. This situation is neatly the exact inverse of that which occurs for the NO–Mo(I)/pyridyl complexes.

EPR Spectra of the Isovalent Polyradicals

Basic Principles of the EPR Spectra. Of the isotopes of molybdenum, about 75% have a nuclear spin I of zero; the remaining 25% have $I = 5/2$. Thus, the EPR spectrum of a paramagnetic molybdenum complex will comprise overlapping singlet (75% of the total intensity, component A in Figure 7) and sextet (25% of the total intensity, B) components at the same g value [Figure 7a]. For both nitrosyl–Mo(I) and oxo–Mo(V) complexes the hyperfine coupling constant A_{Mo} is about 50 G.^{10,14,21}

If, however, the unpaired spin(s) is (are) coupled to two Mo nuclei, then the spectrum consists of a singlet [$I = 0$,

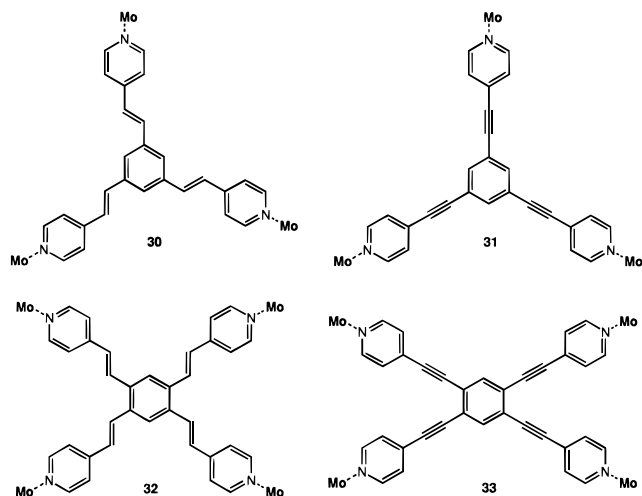


FIGURE 8. Trinuclear and tetranuclear complexes **30–33** [Mo denotes the {Mo(NO)Tp*Cl} fragment].

$I = 0$ nuclear spin combination; 56% probability, component **A**), a sextet [$I = 0, I = 5/2$; 38%, **B**], and a 1:2:3:4:5:6:5:4:3:2:1 undecet [$I = 5/2, I = 5/2$; 6%, **C**], with the hyperfine separation in the multiplets being 25 G, half that observed in mononuclear complexes.^{10,14,21} Such a spectrum can arise in two ways. In a mixed-valence complex [e.g., Mo(I)/Mo(II) or Mo(V)/Mo(VI)] with a single unpaired electron, such a spectrum will arise if the electron is delocalized over both metal centers across the bridging ligand. Second, such a spectrum can arise in a dinuclear complex containing two unpaired electrons [e.g., Mo(I)/Mo(I) or Mo(V)/Mo(V)], even when the electrons are localized on their respective metal centers, provided there is a magnetic exchange interaction between them such that $|J| \gg A_{\text{Mo}}$ (where J is the energy of the exchange interaction and A_{Mo} is the energy of the electron–nucleus hyperfine interaction).²² Such “exchange-coupled” spectra are well-known in nitroxide diradicals, where coupling of both electrons to both nitrogen nuclear spins occurs even across long saturated spacers where there is no question of delocalization of the electrons.^{22b} There are two significant points about this behavior. First, the energy of the hyperfine interaction is very small: the 50 G coupling to Mo nuclei translates to less than 0.01 cm^{-1} , which corresponds to an exchange interaction far too small to be measured by magnetic susceptibility methods, so even a very feeble magnetic exchange interaction will give an exchange-coupled spectrum. Second, the sign of J is irrelevant: ferromagnetic and antiferromagnetic interactions will give the same result as long as $|J|$ is above the very small lower limit.

Nitrosyl–Mo(I) Complexes. All of the dinuclear nitrosyl–Mo(I) complexes mentioned above show an exchange-coupled spectrum [cf. Figure 7b], indicating that $|J| \gg A_{\text{Mo}}$.²² If $|J|$ were much less than A_{Mo} , then the spectrum of Figure 7a would occur from magnetically isolated metal centers. Significantly, this behavior even occurs across the saturated $-\text{CH}_2\text{CH}_2-$ bridge in **13**, indicating that magnetic exchange can occur to some extent through σ -bonds.

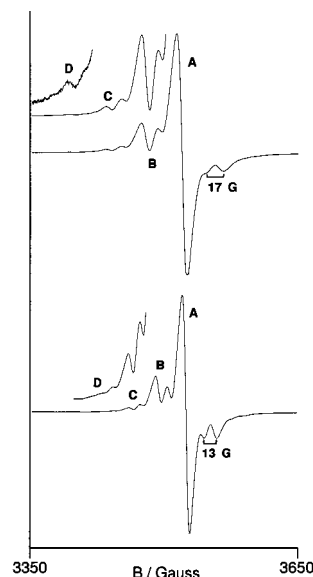
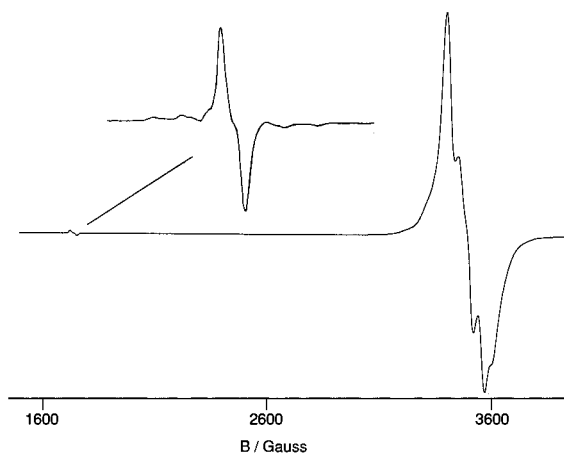
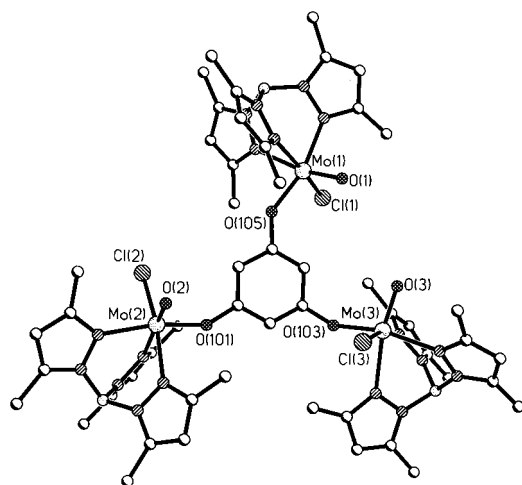


FIGURE 9. EPR spectra for (top) trinuclear and (bottom) tetranuclear complexes of Figure 8.

EPR spectroscopy can also detect magnetic exchange between larger numbers of unpaired spins in higher-nuclearity molybdenum complexes. Attachment of {Mo^I(NO)Tp*Cl} fragments to each pyridyl terminus of the tridentate and tetradentate bridging ligands shown in Figure 8 afforded complexes with three (**30, 31**) or four (**32, 33**) paramagnetic metal fragments linked by a single bridging ligand.²³ The EPR spectra (Figure 9) display the components expected for coupling to three and four Mo nuclei (component **D** in Figure 9 is the 16-fold multiplet arising from coupling to three Mo nuclei, all having $I = 5/2$). The weakest outlying components of the 21-fold multiplet arising from coupling to four Mo nuclei with $I = 5/2$ are not visible in the spectra of **32** and **33**, but the other components are clear, and the reduction of the hyperfine separation to about 17 and 13 G in the trinuclear and tetranuclear complexes (1/3 and 1/4 of the value arising from coupling to one nuclear spin) provides additional confirmation. It is unusual to be able to detect multicenter magnetic exchange in this way; the only other related example is a 22-line spectrum arising from a trinuclear vanadyl complex ($I = 7/2$ for ⁵¹V).²⁴

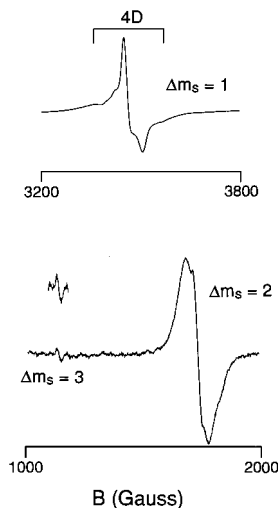
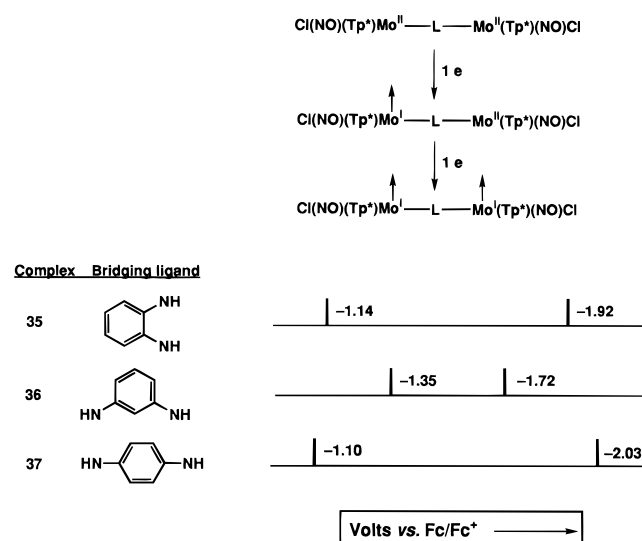
Oxo–Mo(V) Complexes. The EPR spectrum of mononuclear [Mo^V(O)Tp*Cl(OPh)] likewise consists of a superimposed singlet and sextet with a hyperfine coupling A_{Mo} of 50 G.⁸ The dinuclear complexes [{Mo^V(O)Tp*Cl}₂(μ -OO)] give, with the longer bridging ligands, typical exchange-coupled spectra with overlapping 1 + 6 + 11 multiplets and a halved hyperfine separation of 25 G.²⁰ These dinuclear complexes therefore have EPR spectra like those of the dinuclear nitrosyl–Mo(I) complexes, showing the presence of a magnetic exchange interaction between the unpaired electrons with $|J| \gg A_{\text{Mo}}$. As the ligands shorten, the room-temperature spectra become broadened and uninformative, but simultaneously, a half-field $\Delta m_s = 2$ transition becomes apparent at 77 K which provides additional evidence for magnetic exchange (Figure 10). For the trinuclear complex with 1,3,5- $[\text{O}_3\text{C}_6\text{H}_3]^{3-}$

FIGURE 10. EPR spectrum of **28** at 77 K.FIGURE 11. Crystal structure of $[\{\text{Mo}^{\text{V}}(\text{O})\text{Tp}^*\text{Cl}\}_3(\mu\text{-}1,3,5\text{-O}_3\text{C}_6\text{H}_3)]$ (**34**).

as bridging ligand (**34**; Figure 11), the room-temperature spectrum is broad and uninformative but the 77 K spectrum is indicative of a quartet state ($S = 3/2$), with a five-line $\Delta m_s = 1$ transition, and $\Delta m_s = 2$ and (crucially) $\Delta m_s = 3$ transitions at one-half and one-third of the magnetic field of the $\Delta m_s = 1$ transition (Figure 12).¹⁷ $\Delta m_s = 3$ transitions are rarely observed in metal complexes due to their very low intensity,²⁵ and the observation of one here provides confirmation of three-center magnetic exchange in **34** in the absence of hyperfine coupling in the isotropic spectrum.

EPR and IR Spectroscopic Studies of Mixed-Valence States

The combination of electrochemistry, EPR, and infrared spectroscopy proved ideal for examining the mixed-valence states in the dinuclear complexes **35**–**37** (Figure 13); these are diamagnetic Mo(II) (16 valence electron) complexes bridged by dianionic 1,2-, 1,3-, or 1,4-[NHC₆H₄-NH]²⁻ bridges.²⁶ They all undergo two well-separated one-electron reductions to the Mo(II)/Mo(I) and then Mo(I)/Mo(I) species—with the $\Delta E_{1/2}$ value for **36**, with the *meta*-substituted bridge, being less than in **35** and **37**—which allows chemical or electrochemical generation of

FIGURE 12. EPR spectrum of **34** as a frozen glass at 77 K.FIGURE 13. Structures and electrochemical properties of **35**–**37**.

the monoreduced mixed-valence species. Complexes [**35**]⁻ and [**37**]⁻ gave EPR spectra like that in Figure 7b, consistent with the single electron coupling equally to both molybdenum nuclear spins. The electron is therefore delocalized over both metal centers on the EPR time scale (10^{-8} s). In contrast [**36**]⁻ gave a spectrum like that in Figure 7a, consistent with the unpaired electron being localized on one metal center on the EPR time scale. The EPR spectra very clearly show how the localized or delocalized nature of the mixed-valence state depends on the topology of the bridging ligand. For [**35**]⁻ and [**37**]⁻, however, the IR spectra showed two distinct NO stretching frequencies, assignable to localized Mo(II) and Mo(I) termini. These mixed-valence states, which are delocalized on the EPR time scale (10^{-8} s), are therefore localized on the IR time scale (10^{-13} s), which puts upper and lower limits on the exchange rate of the unpaired electron between the two metal centers.²⁶

The pyrazine-bridged complex **1** is unique among the nitrosyl–Mo(I) complexes in that the two Mo(I)/Mo(II) oxidations are separated by 100 mV. Thus, the two mixed-valence states Mo(I)/Mo(0) [**1**⁻, 17e/18e] and Mo(I)/Mo-

(II) [1^+ , 17e/16e] could be generated electrochemically.¹³ The EPR spectrum of [1^-], like those of [35^-] and [37^-], indicated delocalization of the unpaired electron over the pyrazine bridge on the EPR time scale. However, in this case the IR spectrum of [1^-] showed a single NO stretching vibration at 1585 cm^{-1} [*cf.* 1626 cm^{-1} for neutral **1**]; thus, the electron exchange is fast even on the IR time scale (exchange rate $>10^{13}\text{ s}^{-1}$). In contrast the EPR spectrum of the oxidized mixed-valence state [1^+] showed a “localized” EPR spectrum (*cf.* [36^-]), implying that the exchange rate is less than 10^8 s^{-1} . In agreement with this the IR spectrum of the Mo(I)/Mo(II) species showed two NO stretching bands at 1717 and 1608 cm^{-1} , assignable to localized Mo(II) and Mo(I) fragments. The behavior of this complex is exactly consistent with the MO picture in Figure 5a, which predicts that substantial delocalization will occur across the bridging ligand in the reduced species but not in the oxidized species.

Both EPR spectroscopy and IR spectroscopy have been used by others to examine mixed-valence states in dinuclear complexes recently.^{27,28} The combination of *both* techniques in our complexes has proven to be particularly powerful because the ideal spectroscopic characteristics of the component fragments have made the results very easy to interpret, and in some cases has allowed upper and lower limits to be placed on the electron exchange rates.²⁸

Magnetic Susceptibility Studies

Nitrosyl–Mo(I) Complexes. We know from the exchange-coupled EPR spectra of the bis-Mo(I) and bis-Mo(V) complexes that a magnetic exchange interaction is occurring, but this gives no information about the sign or magnitude of J (other than the fact that $|J|$ must exceed a very small lower limit).²² Given the large effect of the bridging ligand structure on electronic interactions between the metals, we investigated how the magnetic exchange interactions (determined from variable-temperature susceptibility measurements) in the same complexes were affected by the bridging ligands. The results for the nitrosyl–Mo(I) complexes with bispyridyl bridging ligands are in Table 1 and have many interesting features.^{15,17}

The most significant result is the alternation in the sign of J as the substitution pattern of the bridging ligand changes from 4,4' to 3,4' to 3,3' for the bipyridine and bis(pyridyl)ethene ligand series. This suggests a spin-polarization mechanism for propagation of the exchange interaction (Figure 14). The unpaired electron on one Mo center polarizes the spin of the electron cloud of the adjacent nitrogen atom in the opposite sense; the next atoms in the sequence will be spin-polarized in the direction opposite that of the N atom, and so on around the bridging ligand. With 4,4'-bipyridine as the bridging ligand (complex **2**) the second Mo spin will be antiferromagnetically coupled to the first one. As the bridging pathway changes in length by one atom to 3,4'-bipyridine (complex **14**), this model predicts that the exchange interaction must become ferromagnetic, which is ob-

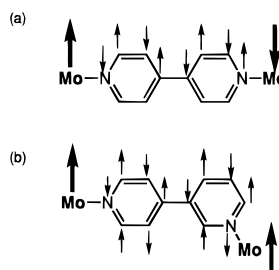


FIGURE 14. The spin-polarization mechanism: (a) antiferromagnetic coupling across 4,4'-bipyridine and (b) ferromagnetic coupling across 3,4'-bipyridine.

served. Changing the path length by an additional atom (to **15**) restores antiferromagnetic exchange.¹⁵

The spin-polarization mechanism arises from the Longuet–Higgins molecular orbital model for conjugated alternant hydrocarbons, which results in ferromagnetic coupling between two radicals separated by an *m*-phenylene bridge.²⁹ The predicted alternation of α and β spin density induced on the intervening atoms³⁰ has been detected and measured in some cases.³¹ A recent result which nicely illustrates the spin-polarization effect in organic diradicals is that a 3,4'-biphenyl bridge promotes ferromagnetic exchange between two unpaired spins, whereas a 3,3'-biphenyl bridge promotes antiferromagnetic exchange (*cf.* the effects of 3,4'-bipyridine and 3,3'-bipyridine in our complexes, Figure 14).³²

The second notable feature of these results is the dependence of J on the conformation of the bridging ligand.^{15,17} Comparison of **2** (26° twist between the pyridyl rings according to a molecular mechanics calculation) and **10** (90° twist between the rings) shows that the magnitude of J decreases by about 90% as the two halves of the ligand approach orthogonality. It follows that the spin-polarization process is largely transmitted through the delocalized π -system of the bridging ligand. The same effect is present less obviously when comparing the (twisted) dipyriddy bridging ligands (**2**, **14**, and **15**) with their planar bis(pyridyl)ethene analogues (**3**, **16**, and **17**, respectively). Thus, on moving from 3,4'-bipyridine (**14**; twist angle 35°) to the planar bis(pyridyl)ethene analogue (**16**), the expected decrease in J because of the increased ligand length is more than offset by the change to planarity, such that the longer planar ligand allows a stronger ferromagnetic coupling than the shorter twisted one. When 4,4'-bipyridine (**2**; twist angle 26°) is compared with bis(4-pyridyl)ethene (**3**), the change in conformation is less significant and J therefore decreases as the ligand lengthens.¹⁵

Oxo–Mo(V) Complexes. The same patterns of magnetic behavior appear in the dinuclear oxo–Mo(V) complexes with bisphenolate (“OO”) bridging ligands (Table 2).¹⁷ First, between **24** (*para*-substituted bridge) and **28** (*meta*-substituted bridge), the exchange interaction changes sign from antiferromagnetic to ferromagnetic. Second, increasing the length of the bridge (**24**, **25**) results in a decrease in the magnitude of J . Third, imposing a twist between the two halves of the bridge (**25**, **29**) results in a substantial decrease in the magnitude of J .

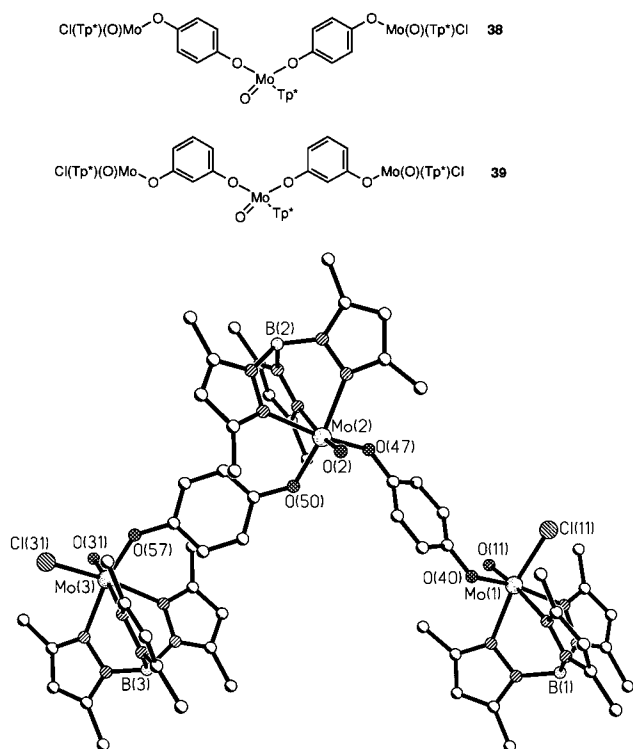


FIGURE 15. Structural formulas of **38** and **39**, and the crystal structure of **38**.

The spin-polarization principle also works for the trinuclear complexes **34** (Figure 11), **38**, and **39** (Figure 15). In **34** the bridging ligand 1,3,5-benzenetriolate results in a *meta* geometric relationship between each pair of oxo-Mo(V) centers. Complexes **38** and **39** are linear chains, with 1,4- and 1,3-benzenediolate bridges between adjacent pairs of metals. On the basis of spin polarization, we would expect **34** to have a quartet ($S = 3/2$) ground state with all metal centers ferromagnetically coupled. This was suggested by the EPR spectrum (Figure 12) and confirmed by magnetic susceptibility measurements ($J = +14.4 \text{ cm}^{-1}$).¹⁷ For **38** and **39**, application of the spin-polarization principle predicts ground states of $S = 1/2$ (spin arrangement $\uparrow\downarrow$) and $S = 3/2$ (spin arrangement $\uparrow\uparrow$) arising from antiferromagnetic and ferromagnetic coupling, respectively, between adjacent spins, and this was also confirmed with $J = -44$ and $+4.5 \text{ cm}^{-1}$, respectively.³³

The spin-polarization mechanism for magnetic exchange has therefore been confirmed for two independent [nitrosyl-Mo(I) and oxo-Mo(V)] sets of complexes, and holds for trinuclear as well as dinuclear complexes. The potential for extending it to larger systems is obvious.

Conclusions

The $\{\text{Mo}^{\text{I}}(\text{NO})\text{Tp}^*\}$ and $\{\text{Mo}^{\text{V}}(\text{O})\text{Tp}^*\}$ fragments have proved to be ideal for the study of long-distance electronic and magnetic interactions across conjugated bridging ligands. Not only are the interactions exceptionally strong because of the nearly ideal matching in both symmetry and energy terms of the relevant metal orbitals with those of the bridging ligands, but the complexes are amenable to study by a wide range of techniques (voltammetry, EPR

and IR spectroscopy, and magnetic susceptibility) which have complemented each other and allowed electrochemical and magnetochemical properties to be studied in tandem. We have shown how electronic and magnetic interactions between two or more metal centers are determined by the nature of the bridging ligand, and the results should be of fundamental interest for the design of future multinuclear compounds in the areas of molecular electronics and magnetic materials.

We express our thanks to all of the co-workers who have collaborated in this area over the past few years; their names appear in the reference list below. Particular thanks go to Dr. Chris Jones (University of Birmingham) who played a major role in much of the early work described here; to Dr. John Maher (University of Bristol) for the EPR measurements, and to Professor Dante Gatteschi (University of Firenze) and his colleagues for the magnetic susceptibility measurements.

References

- (1) Ward, M. D. Metal-metal interactions in binuclear complexes exhibiting mixed-valency; molecular wires and switches. *Chem. Soc. Rev.* **1995**, 121-134.
- (2) (a) Ward, M. D. Current developments in molecular wires. *Chem. Ind.* **1996**, 568-573. (b) Ward, M. D.; Current developments in molecular switches. *Chem. Ind.* **1997**, 640-645.
- (3) (a) Kahn, O. *Molecular Magnetism*; VCH Publishers, Inc.: New York, 1993. (b) Bushby, R. J.; Paillaud, J.-L. Molecular magnets. In *Introduction to Molecular Electronics*; Petty, M. C., Bryce, M. R., Bloor, D., Eds.; Edward Arnold: London, 1995, pp 72-91.
- (4) (a) Goodenough, J. B. Theory of the role of covalence in the perovskite-type manganites $[\text{La}_x\text{M}(\text{II})\text{MnO}_3]$. *Phys. Rev.* **1955**, *100*, 564-573. (b) Goodenough, J. B. An interpretation of the magnetic properties of the perovskite-type mixed crystals $\text{La}_{(1-x)}\text{Sr}_x\text{CoO}_{(3-x)}$. *J. Phys. Chem. Solids* **1958**, *6*, 287-297. (c) Kanamori, J. Superexchange interaction and symmetry properties of electron orbitals. *J. Phys. Chem. Solids* **1959**, *10*, 87-98. (d) Ginsberg, A. P. Magnetic exchange in transition-metal complexes, VI: aspects of exchange coupling in magnetic cluster complexes. *Inorg. Chim. Acta Rev.* **1971**, *5*, 45-68.
- (5) (a) Kahn, O. Magnetism of the heteropolymetallic systems. *Struct. Bonding* **1987**, *68*, 89-167. (b) Gordon-Wylie, S. W.; Bominaar, E. L.; Collins, T. J.; Workman, J. M.; Claus, B. L.; Patterson, R. E.; Williams, S. A.; Conklin, B. J.; Yee, G. T.; Weintraub, S. T. Ligand design for securing ferromagnetic exchange coupling in multinuclear complexes. *Chem. Eur. J.* **1995**, *1*, 528-537. (c) Lloret, F.; De Munno, G.; Julve, M.; Cano, J.; Ruiz, R.; Caneschi, A. Spin Polarization and Ferromagnetism in Two-Dimensional Sheetlike Cobalt(II) Polymers: $[\text{Co}(\text{L})_2(\text{NCS})_2]$ (L = Pyrimidine or Pyrazine). *Angew. Chem., Int. Ed. Engl.* **1998**, *37*, 135-138.
- (6) (a) Miller, J. S.; Epstein, A. J. Organic and organometallic molecular magnetic materials - designer magnets. *Angew. Chem., Int. Ed. Engl.* **1994**, *33*, 385-415. (b) Iwamura, H. Approaches from super-high-spin molecules to organic ferromagnets. *Pure Appl. Chem.* **1993**, *65*, 57-64. (c) Rajca, S. Organic diradicals and polyradicals: from spin coupling to magnetism. *Chem. Rev.* **1994**, *94*, 871-893. (d) Rajca, S.; Rajca, A. Novel high-spin molecules: π -conjugated polyradical polyanions. Ferromagnetic

- spin coupling and electron localization. *J. Am. Chem. Soc.* **1995**, *117*, 9172–9179. (e) Yoshizawa, K.; Hoffman, R. Potential linear-chain organic ferromagnets. *Chem. Eur. J.* **1995**, *1*, 403–413. (f) Iwamura, H.; Koga, N. Studies of organic di-, oligo- and polyradicals by means of their bulk magnetic properties. *Acc. Chem. Res.* **1993**, *26*, 346–351.
- (7) (a) McWhinnie, S. L. W.; Jones, C. J.; McCleverty, J. A.; Collison, D.; Mabbs, F. E. Synthesis and characterization of 17-electron species of nitrosyl(tris-3,5-dimethylpyrazolylborato)molybdenum. *Polyhedron* **1992**, *11*, 2639–2643. (b) Das, A.; Drane, A. S.; McCleverty, J. A. Alkoxy, amido and thiolato complexes of tris(3,5-dimethylpyrazolyl)borato(nitrosyl)molybdenum fluoride, chloride and bromide. *Polyhedron* **1983**, *2*, 53–57. (c) Charsley, S. M.; Jones, C. J.; McCleverty, J. A.; Neaves, B. D.; Reynolds, S. J.; Denti, G. Monometallic, homo- and heterobimetallic complexes based on redox-active tris(3,5-dimethylpyrazolyl)borato molybdenum and tungsten nitrosyls. Part 7. Compounds containing strongly interacting redox centres derived from *para*-substituted anilines and phenols. *J. Chem. Soc., Dalton Trans.* **1988**, 293–299.
 - (8) Cleland, W. E., Jr.; Barhrt, K. M.; Yamanouchi, K.; Collison, D.; Mabbs, F. E.; Ortega, R. B.; Enemark, J. H. Syntheses, structures and spectroscopic properties of six-coordinate mononuclear oxo-molybdenum(V) complexes stabilized by the hydrotris(3,5-dimethyl-1-pyrazolyl)borate ligand. *Inorg. Chem.* **1987**, *26*, 1017–1025.
 - (9) Westcott, B. L.; Enemark, J. H. Formal oxidation states vs. π -effects in isostructural low-symmetry $[\text{MoNO}]^{3+}$ and $[\text{MoO}]^{3+}$ complexes: a photoelectron spectroscopy study. *Inorg. Chem.* **1997**, *36*, 5404–5405.
 - (10) McWhinnie, S. L. W.; Jones, C. J.; McCleverty, J. A.; Collison, D.; Mabbs, F. E. EPR and electrochemical studies of bimetallic seventeen-electron molybdenum species exhibiting unusually large interactions across bipyridyl bridging ligands. *J. Chem. Soc., Chem. Commun.* **1990**, 940–942.
 - (11) Sutton, J. E.; Taube, H. Metal to metal interactions in weakly coupled mixed-valence complexes based on ruthenium amines. *Inorg. Chem.* **1981**, *20*, 3125–3134.
 - (12) Thomas, J. A.; Jones, C. J.; McCleverty, J. A.; Collison, D.; Mabbs, F. E.; Harding, C. J.; Hutchings, M. G. An EPR, magnetic and electrochemical study of electron-exchange and intermetallic interactions through polyene bridges. *J. Chem. Soc., Chem. Commun.* **1992**, 1796–1798.
 - (13) Wlodarczyk, A.; Doyle, G. A.; Maher, J. P.; McCleverty, J. A.; Ward, M. D.; Thomas, J. A.; Jones, C. J. Mixed-valency by oxidation and reduction: a molybdenum-based super-Creutz-Taube ion. *Chem. Commun.* **1997**, 769–770.
 - (14) Das, A.; Maher, J. P.; McCleverty, J. A.; Navas, J. A.; Ward, M. D. Metal–metal interactions across symmetrical bipyridyl bridging ligands in binuclear complexes containing two seventeen-electron molybdenum centres. *J. Chem. Soc., Dalton Trans.* **1993**, 681–686.
 - (15) Cargill Thompson, A. M. W.; Gatteschi, D.; McCleverty, J. A.; Navas, J. A.; Rentschler, E.; Ward, M. D. Effects of systematic variation in bridging ligand structure on the electrochemical and magnetic properties of a series of dinuclear molybdenum complexes. *Inorg. Chem.* **1996**, *35*, 2701–2703.
 - (16) Hock, J.; Cargill Thompson, A. M. W.; McCleverty, J. A.; Ward, M. D. Some new di-pyridyl and diphenol bridging ligands containing oligothiényl spacers, and their dinuclear molybdenum complexes: electrochemical, spectroscopic and luminescence properties. *J. Chem. Soc., Dalton Trans.* **1996**, 4257–4263.
 - (17) Ung, V. A.; Cargill Thompson, A. M. W.; Bardwell, D. A.; Gatteschi, D.; Jeffery, J. C.; McCleverty, J. A.; Totti, F.; Ward, M. D. The roles of bridging ligand topology and conformation in controlling exchange interactions between paramagnetic molybdenum fragments in dinuclear and trinuclear complexes. *Inorg. Chem.* **1997**, *36*, 3447–3454.
 - (18) Creutz, C.; Taube, H. Binuclear complexes of ruthenium amines. *J. Am. Chem. Soc.* **1973**, *95*, 1086–1094.
 - (19) Richardson, D. E.; Taube, H. Electronic interactions in mixed-valence molecules as mediated by organic bridging groups. *J. Am. Chem. Soc.* **1983**, *105*, 40–51.
 - (20) Ung, V. A.; Bardwell, D. A.; Jeffery, J. C.; Maher, J. P.; McCleverty, J. A.; Ward, M. D.; Williamson, A. Dinuclear oxo-molybdenum(v) complexes with bisphenol bridging ligands: syntheses and structures, and electrochemical and EPR spectroscopic properties. *Inorg. Chem.* **1996**, *35*, 5290–5299.
 - (21) Das, A.; Jeffery, J. C.; Maher, J. P.; McCleverty, J. A.; Schatz, E.; Ward, M. D.; Wollermann, G. Mono- and bi-nuclear molybdenum and tungsten complexes containing asymmetric bridging ligands: the effects of ligand conjugation and conformation on metal–metal interactions. *Inorg. Chem.* **1993**, *32*, 2145–2155.
 - (22) (a) Reitz, D. C.; Weissman, S. I. Spin exchange in biradicals. *J. Chem. Phys.* **1960**, *33*, 700–704. (b) Brière, R.; Dupeyre, R.-M.; Lemaire, H.; Morat, C.; Rassat, A.; Rey, P. Nitroxydes XVII: biradicaux stables du type nitroxyde. *Bull. Soc. Chim. Fr.* **1965**, *11*, 3290–3297.
 - (23) Amoroso, A. J.; Cargill Thompson, A. M. W.; Maher, J. P.; McCleverty, J. A.; Ward, M. D. Di-, tri- and tetranuclear pyridyl ligands which facilitate multi-centre magnetic exchange between paramagnetic molybdenum centres. *Inorg. Chem.* **1995**, *34*, 4828–4835.
 - (24) (a) Parker, C. C.; Reeder, R. R.; Richards, L. B.; Rieger, P. H. A novel vanadyl pyrophosphate trimer. *J. Am. Chem. Soc.* **1970**, *92*, 5230–5231. (b) Hasegawa, A. Electron spin resonance of a trinuclear vanadyl pyrophosphate complex. *J. Chem. Phys.* **1971**, *55*, 3101–3104.
 - (25) (a) Siedle, A. R.; Padula, F.; Baranowski, J.; Goldstein, C.; De Angelo, M.; Kokoszka, G. F.; Azevedo, L.; Venturini, E. L. Transmission of magnetic interactions in a molecular metal oxide cluster. *J. Am. Chem. Soc.* **1983**, *105*, 7447–7448. (b) Kokoszka, G. F.; Padula, F.; Goldstein, C.; Venturini, E. L.; Azevedo, L.; Siedle, A. R. Magnetic interactions in a copper(II) trimer encapsulated in a molecular metal oxide cluster. *Inorg. Chem.* **1988**, *27*, 59–62. (c) Francesconi, L. C.; Corbin, D. R.; Hendrickson, D. N.; Stucky, G. D. Binuclear bis(η^5 -methylcyclopentadienyl)titanium(III) complexes bridged by the dianion of 2,4-dithiopyrimidine and related dianions: magnetic and EPR properties. *Inorg. Chem.* **1979**, *18*, 3074–3080.

- (26) Wlodarczyk, A.; Maher, J. P.; McCleverty, J. A.; Ward, M. D. Dinuclear molybdenum complexes containing benzene-diamido and dianilido bridges: mixed-valence behaviour and electrochemical interactions. *J. Chem. Soc., Dalton Trans.* **1997**, 3287–3298.
- (27) (a) Le Narvor, N.; Lapinte, C. First C₄-bridged mixed-valence iron(II)-iron(III) complex delocalized on the infra-red timescale. *J. Chem. Soc., Chem. Commun.* **1993**, 357–359. (b) Seyler, J. W.; Weng, W.; Zhou, Y.; Gladysz, J. A. An isolable organometallic cation radical in which a C₄-chain conducts charge between two chiral and configurationally stable rhenium termini. *Organometallics* **1993**, *12*, 3802–3804.
- (28) (a) Etzenhouser, B. A.; Cavanaugh, M. D.; Sprugeon, H. N.; Sponsler, M. B. Mixed-valence diiron complexes with butadienyl bridges. *J. Am. Chem. Soc.* **1994**, *116*, 2221–2222. (b) Pierce, D. T.; Geiger, W. E. Mixed-valent interactions in rigid dinuclear systems: electrochemical and spectroscopic studies of Cr^ICr⁰ ions with controlled torsion of the biphenyl bridge. *Inorg. Chem.* **1994**, *33*, 373–381. (c) Bruns, W.; Kaim, W.; Waldhör, E.; Krejčík, M. Spectroelectrochemical characterization of a pyrazine-bridged mixed-valent (4d⁵/4d⁶) organometallic analogue of the Creutz-Taube ion. *J. Chem. Soc., Chem. Commun.* **1993**, 1868–1869.
- (29) Longuet-Higgins, J. C. Some studies in molecular orbital theory (I). Resonance structures and molecular orbitals in unsaturated hydrocarbons. *J. Chem. Phys.* **1950**, *18*, 265–274.
- (30) (a) Karafiloglou, P. Through-bond interaction of two radical centres: analysis of the spin-polarization and related interactions in linear π -diradicals. *J. Chem. Phys.* **1985**, *82*, 3728–3740. (b) Ovchinnikov, A. A. Multiplicity of the ground state of large alternant organic molecules with conjugated bonds. *Theor. Chim. Acta* **1978**, *47*, 297–304.
- (31) (a) Okamoto, M.; Teki, Y.; Takui, T.; Kinoshita, T.; Itoh, K. Spin density distribution of an organic high-spin molecule, biphenyl-3, 3'-bis(phenylmethylene), as studied by ¹H ENDOR and a UHF Hubbard calculation. *Chem. Phys. Lett.* **1990**, *173*, 265–270. (b) Takui, T.; Kita, S.; Ichikawa, S.; Teki, Y.; Kinoshita, T.; Itoh, K. Spin distribution of organic high-spin molecules as studied by ENDOR/TRIPLE. *Mol. Cryst. Liq. Cryst.* **1989**, *176*, 67–76.
- (32) (a) Rajca, A.; Rajca, S. Intramolecular antiferromagnetic vs. ferromagnetic spin-coupling through the biphenyl unit. *J. Am. Chem. Soc.* **1996**, *118*, 8121–8126. (b) Minato, M.; Lahti, P. M.; van Willigen, H. Models for intramolecular exchange in organic π -conjugated open-shell systems: a comparison of three non-Kekulé biphenyldinitrenes. *J. Am. Chem. Soc.* **1993**, *115*, 4532–4539.
- (33) Ung, V. A.; Couchman, S. M.; Jeffery, J. C.; McCleverty, J. A.; Ward, M. D.; Totti, F.; Gatteschi, D. Electrochemical and magnetic exchange interactions in trinuclear chain complexes containing oxo-Mo(V) fragments as a function of the topology of the bridging ligand. *Inorg. Chem.*, submitted for publication.

AR970315S